Molecular Modeling of DNA Cross-linking Analogues Based on the Azinomycin Scaffold

Stefano Alcaro,*,† Francesco Ortuso,† and Robert S. Coleman‡

Dipartimento di Scienze Farmacobiologiche, Università "Magna Græcia" di Catanzaro, I-88021 Roccelletta di Borgia, Catanzaro, Italy, and Department of Chemistry, The Ohio State University, 100 West 18th Avenue, Columbus, Ohio 43210

Received November 10, 2004

In this work, we present molecular modeling studies carried out using six DNA sequences and six azinomycin analogues, including the naturally occurring compound azinomycin B, selected on the basis of known cell cytotoxicity and structural analogies (epoxide and aziridine alkylating moieties). Among several computational methods the Stochastic Dynamics with Energy Minimization (SDEM) approach yielded results superior to the others with the natural compound ($r^2 > 0.9$) and was adopted for studying other DNA adducts, obtaining good correlation between the average theoretical cross-linking properties and the antitumor activity scale. As a result, some interesting SAR considerations have been highlighted and a cross-linking conformation different from that of the azinomycin was identified in a less potent, simplified analogue.

INTRODUCTION

The natural product azinomycin B, **1**, and the structurally related agents (Figure 1) are antitumor agents[1] that exhibit both in vitro cytotoxicity and in vivo antitumor activity.[2,3] Azinomycin B appears to exert its biological activity by the formation of covalent interstrand cross-links[4] in duplex DNA, via the electrophilic epoxide and aziridine rings. However a detailed biological evaluation of these agents has been hampered by chemical instability and poor availability from natural sources. Cross-linking occurs within the major groove via the N7 alkylation of two purine bases.[5,6] This molecular mechanism of action and effective antitumor activity makes the azinomycins attractive targets for synthetic[7,8] and mechanistic studies.[5,6]

In our earliest study of azinomycins we developed force-field parameters and described Monte Carlo conformational searching of the natural agents.[9] Because of the large number of populated conformers, we developed filtering protocols based on a distance and vector analysis of the cross-linking site in duplex DNA in order to analyze low energy conformers. In that work we concluded that azinomycin A and B were highly preorganized for DNA cross-linking.

The interactions of azinomycin B with duplex DNA are challenging to study using computational methods because of the conformationally mobile nature of the molecule. In another publication[10] we approached the interaction study considering one DNA sequence reported to undergo a high degree of cross-linking by the natural compound.[5] In agreement with the experimental results, we found that only one cross-linking path is preferred, in particular with reaction I, the aziridine attack to the purine N7 in the "bottom" position of the triplet followed by the reaction II, the "top" interstrand alkylation of the epoxide as shown in Scheme 1.

The selectivity of the natural compound toward specific DNA sequences was the object of our previous investigation.[11] High levels of sequence selectivity in covalent cross-link formation is characteristic of azinomycin B, as described,[6] and knowledge about the structural origins of this selectivity is essential for the rational design of second generation azinomycin analogues. The molecular model developed was able to discriminate between the cross-linking activity of azinomycin toward four DNA duplex sequences, in excellent correlation with the qualitative experimental data.[6] Detailed insights about the driving interaction in the cross-linking mechanism were obtained. A second and equally important conclusion was that the conformational properties of the DNA monoalkylation species, denoted aziridine bottom (MAB), represents the crucial step for explaining the entire cross-linking mechanism of action. More recently, this observation was supported by the experimental evidence of a lack of intercalative role of the naphthoate moiety in the azinomycin B mechanism of action[12] and the quantitation of cross-linking reactivity of the natural compound toward six DNA duplexes.[13]

Our aim in the present studies was to derive a molecular model useful for design of more potent/selective drug analoges. We have extended the previous work, selecting known azinomycin B analogues from the literature based on the availability of in vitro antitumor activity and the presence of the essential chemical moieties (the epoxide and the aziridine) involved in the cross-linking mechanism and the naphthoate ring.[3] Six compounds with these characteristics (Figure 1), including the azinomycin B, were identified and adopted as a training set for the QSAR study that was based on the theoretical cross-linking ability. The biological activity (expressed as IC_{50} values) in two tumor cell lines prompted us to consider all possible DNA triplets matching the general formula 5′-d(PuNPy)-3′ as target receptors (Pu = purine, Py = pyrimidine). Even if the two sets of cell line inhibition activities are different, azinomycin B is referenced for both with comparable values of 1.6 and 0.8

* Corresponding author phone: (+39)0961-391157; fax: (+39)0961-391490; e-mail: alcaro@unicz.it.
† Università "Magna Græcia" di Catanzaro.
‡ The Ohio State University.

10.1021/ci0496595 CCC: $30.25
Published on Web 03/31/2005

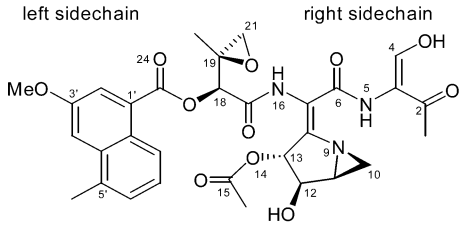

1 (Azinomicyn B) $IC_{50}^{a} = 1.6\ \mu M$ $IC_{50}^{b} = 0.8\ \mu M$

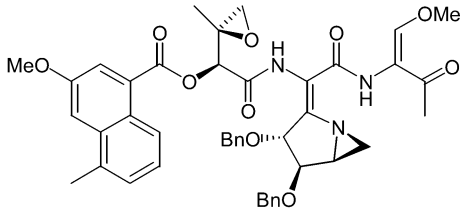

2 (205441-75-4) $IC_{50}^{a} = 0.5\ \mu M$

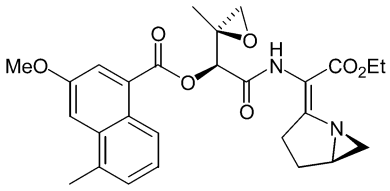

3 (157825-34-8) $IC_{50}^{a} = 0.0047\ \mu M$

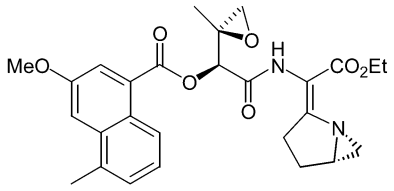

4 (157904-55-7) $IC_{50}^{a} = 0.0073\ \mu M$

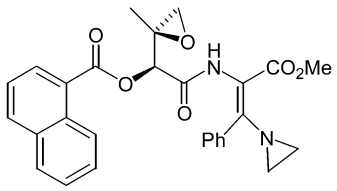

5 (167985-96-8) $IC_{50}^{b} = 4.39\ \mu M$

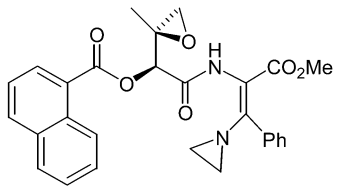

6 (167985-95-7) $IC_{50}^{b} = 12.4\ \mu M$

Figure 1. Chemical structures and IC50 of azinomycin B (**1**) and related compounds. In parentheses the Chemical Abstract Service numbers of compounds **2**−**6** are reported. [a]Cytotoxic activity against P388 cell lines.[1,2,4] [b]Cytotoxic activity against HCT116 cell lines.[4]

Scheme 1. Two Steps in the Cross-linking Mechanism of Azinomycin B and a Generic DNA Triplet, Defined as 5′-Pu-N-Py-3′ [a]

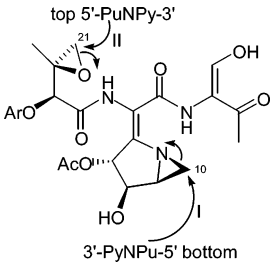

[a] Pu, Py, and N respectively represent purine, pyrimidine and any nucleotides.

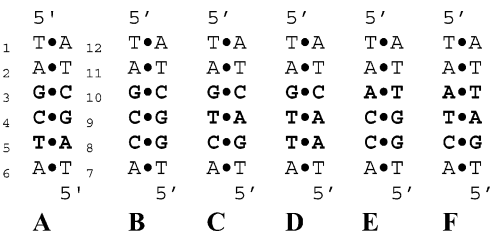

Figure 2. Structure of duplex DNA sequences **A, B, C, D, E,** and **F** modeled in B-form conformation with nucleotide numbering scheme.

μM, respectively, against P388 murine leukemia and HCT116 human colon carcinoma cell lines. The cytotoxicity of the six compounds can be summarized as follows:

$$\mathbf{3} > \mathbf{4} >> \mathbf{2} > \mathbf{1} > \mathbf{5} > \mathbf{6}$$

To create a molecular model most consistent with existing experimental data, we considered six DNA duplexes possessing a broad spectrum of cross-linking reactivity.[6] The length of the DNA fragments was standardized to 6 nucleotides and the first, second, and sixth nucleotides were chosen adjacent to receptor triplets according to a literature reference.[5] The six duplexes and their complementary strands are shown in Figure 2.

The computational model was carried out by different intensive computational protocols focusing on the MAB monoadduct between the six cross-linking agents (Figure 1) and the six duplex DNA sequences (Figure 2). The selection of the most appropriate of the four computational methods was made by analyzing the theoretical cross-linking properties of **1**·DNA monoadducts with different filtering criteria and comparing them with the DNA sequence-dependent experimental decreasing reactivity[13] of azinomycin B toward each 6-mer duplex, as follows:

$$\mathbf{B} >> \mathbf{A} > \mathbf{C} >> \mathbf{D} \geq \mathbf{E} > \mathbf{F}$$

The best computational method was extended to study DNA monoadducts with **2**−**6**. Three computational protocols reproduced the antitumor activity scale of the six compounds with good correlation. The analysis of the three-dimensional structure of the most stable monoadduct allowed identification of the putative bioactive conformation of the most active compounds.

METHODS

The computational work focused on the most important step of the cross-linking mechanism of action of azinomycin B analogues: formation of the MAB monoadducts with the DNA. The other three possible monoadducts[14] with the DNA triplets were discarded because they gave no correlation with the experimental reactivity of **1** in our previous computational experiments.[10,11]

Sequences **A**−**F** were created in B-form conformation placing Na^{+} counterions 2.5 Å from each anionic oxygen of

Chart 1: General Structure of the Charged Monoadduct Obtained Opening the Aziridine Moiety after the Purine Alkylation

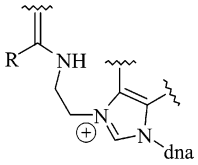

the phosphates, thereby neutralizing the charge of the DNA backbone and minimizing unrealistic electrostatic interactions between the agents and phosphates. This operation was performed with the Silicon Graphic version 5.5 MacroModel package,[15] while all the energy calculations were carried out with BatchMin Linux version 7.2[16] distributed on a 14 Intel processor cluster.

Starting Models and Energy Evaluation. The monoadduct building was performed by opening the aziridine ring of compounds **1**−**6** and connecting the methylene carbon to the nucleophilic N7 purine atom of the eight **A**−**F** duplex nucleotides, following the same procedure as in our previous study (Chart 1).[11]

These starting structures are positively charged due to the N7 alkylation, requiring the adoption of an AMBER* force field modification for N7 alkylated nucleotides.[11] In compounds **5** and **6** the stereochemistry of nitrogen of the ring-opened aziridine moiety was not defined, but the geometry of this atom was considered trigonal due the resonance effect of the α sp^2 carbon.

All computational experiments fixed the DNA and counterions in the monoadduct simulation using a force constant of 24 kcal/mol.[17] To compare our results with previous work,[11] the energy evaluation of the structures was carried out using the same treatment.[18] The solvation effect was taken into account applying the GB/SA water implicit model as implemented in version 7.2 of MacroModel.

Conformational Search. The conformational search of the **1**·DNA monoadducts was carried out using different computational methods with the aim to determine the most reasonable one for the correlation study between the theoretical cross-linking properties and existing experimental data.[13] Monte Carlo (MC), Stochastic Dynamics (SD), Stochastic Dynamics + Energy Minimization (SDEM), and Monte Carlo Stochastic Dynamic mixed mode (MCSD) methods were used.[19]

Starting structures were modeled using a Monte Carlo conformational search of the adducts, randomizing all 18 rotatable torsional angles on the **1** fragment including the purine N7-agent bond. Five thousand conformations were generated and minimized with the Polak-Ribiere Conjugate Gradient (PRCG) and our modified AMBER* force field[11] directly in GB/SA water model (≤ 10 000 iterations). Convergence in the Monte Carlo search was judged complete if the global minimum was found more than one time, and if in the final portion of the calculation, the random conformer generation was not able to reach deeper energy wells in the conformational space. Conformations >12 kcal/mol above the minimum were discarded from the Monte Carlo search. The ensemble of each **1**-DNA adduct was considered for the correlation study with the experimental cross-linking data.

To carry out a refinement of the conformational exploration, the global minimum of each DNA monoadduct was submitted the Stochastic Dynamics method under the following conditions: (a) equilibration time 1.5 ps at 300 K; (b) 5000 ps of simulation time at 300 K; (c) time step = 1.5 fs; and (d) 250 conformations stored. The same constraints, force field, and solvation model have been adopted previously for such simulations. Convergence in the Stochastic Dynamic simulation was judged complete by analyzing the graph of root-mean-square (RMS) deviations of the 250 stored structures with respect to the starting structure obtained by MC method (see Supporting Information, Figure 5). The SD ensemble of each **1**·DNA adduct was considered for the correlation study with the experimental data.

To make a direct energy comparison of the conformers obtained by the MC and the SD method, the collection of SD conformations was submitted to a multiminimization step under the following conditions: maximum PRCG iterations ≤ 10 000, conformational deduplication equal to 0.05 kcal/Å·mol, and 24 kcal/mol DNA and sodium constraint. The SDEM ensemble obtained for each adduct was considered for the correlation study with the experimental data.

In the mixed-mode MCSD, rotatable bonds were implemented exactly as set in the MC search as well as the SD simulation length of 5000 ps at 300 K. Similarly, the obtained MCSD ensemble of 100 conformers for each adduct was considered for the correlation study with the experimental cross-linking data.

With the goal to identify computational protocols best able to reproduce the antitumor activity scale of the known azinomycin analogues, comparison of the different four methods allowed selection of the most appropriate for studying the **2**−**6** monoadducts with the six DNA sequences.

Cross-linking Probability and Correlation with Experimental Data. To find the most appropriate computational protocol for the design of new azinomycin analogues, the best correlation between the direct cross-linking activity of **1** and the DNA sequences[13] was first considered. The cross-linking probability of the six monoadducts modeled for each conformational ensemble was evaluated with the same filtering criterion of the previous DNA-azinomycin studies.[10,11] The distance *d* and attack angle *a* between the epoxide methylene carbon of **1**−**6** compounds and the purine N7 of the third nucleotide were systematically varied within a range of accepted values.[20] For each distance ≤ *d* and angle ≥ *a* we evaluated the cross-linking probability *p* by summation of the Boltzmann probability computed at 300 K of those minimum energy conformations satisfying the filtering criteria. The comparison with the experimental activity of **1** against the six DNA sequences allowed identification of the best computational method.

The second step of the correlation analysis was carried out making some assumptions and should be considered as a provisional approach to developing a computational protocol reasonably appropriate for the drug design of new azinomycin analogues. The first assumption is that cytotoxic activity is related to the cross-linking properties of each compound **1**−**6** toward the **A**−**F** sequences of the tumor cell line DNA. This statement justifies the calculation of the averaged cross-linking probability p_{A-F} for each compound and its direct comparison with the pIC_{50}. The second assumption is that the cell line data are comparable to each other, and consequently the qualitative reactivity scale reported in the Introduction can be accepted. While neither

of these assumptions are strictly true quantitatively, it is reasonable to assume such direct correlations within a closely related series of compounds. No other properties of compounds **1**−**6** such as stability and bioavailability at the DNA receptor site are considered in our computational model.

The best computational method found in the previous step was applied in the monoadduct molecular modeling of all 36 possible DNA sequence-compound combinations. The same systematic approach was used to identify the best computational protocol (distance and angle filtering criterion) correlating with the known inhibition scale.

RESULTS AND DISCUSSION

The results have been initially evaluated considering the convergence in the conformational search of **1**-DNA monoadducts with the four different computational approaches.

For those methods including the minimization and deduplication procedures (MC and SDEM) we took into account the conformational distribution within the first 12 kcal/mol above the global minima and the average number of duplicates (AD), that can be considered as a descriptor of evaluating the convergence quality in the search. Duplications occur when a conformation differs to another generated during the simulation with an RMS in the atomic coordinates lower than 0.25 Å. Typically, AD values close to 1 indicate a poor exploration, while numbers higher than 2, especially in complicated systems with several rotatable bonds, can be related to a sufficiently extended conformational search.[21] The lowest AD values were found with sequences **F** respectively equal to 2.34 in MC search and 9.79 in the SDEM multiminimization (see Supporting Information, Table 3). In all other cases the AD numbers found were much higher than 2.34. So we concluded that our simulations were acceptable for the conformational space of these adducts.

For the other two methods (SD and MCSD) we evaluated the RMS deviation, computed considering the drug only, with respect to the original starting structures, which corresponded to the global minimum conformers obtained by the MC search. In all cases, we analyzed the conformational search as complete by the RMS stabilization around 1000 ps for both SD and MCSD simulations (see Supporting Information, Figures 5 and 6).

We then proceeded with the energy evaluation of the global minima adduct conformers found with the four computational approaches (see Supporting Information, Table 4).

The first step in the evaluation of the computational conditions (conformational search method) involved examining the ability to reproduce the experimentally determined cross-linking of azinomycin B activity[13] with respect to the six naked oligo-duplex DNA sequences (Table 1).

The correlation square factor r^2, calculated according to the Bravais-Pearson equation, was used as the key parameter of evaluation of the computational procedure. Despite the good r^2 of the MC generated ensemble, the computational data in Table 1 clearly indicate poor correlation with reality, demonstrating almost zero probability to afford cross-links for all DNA monoadducts.

Similar consideration can be made for the MCSD method. Even the most highly cross-linked sequence **B** was correctly located as the most reactive by the SD theoretical cross-link activity, the square correlation factor r^2 was not satisfactory due to the incorrect prediction of other **1**-DNA monoadducts.

Table 1. Best Filtering Conditions (Distance *d* and Attack Angle *a* Thresholds) Based on the Highest Square Correlation Factor r^2 between the Theoretical Cross-linking Probability with Different Ensembles of Each 1-DNA Adduct and the Experimental Cross-linking Activity XL[13]

	cross-linking probability per ensemble				
DNA adduct	MC	SD	SDEM	MCSD	XL %
1-A	0.00	0.00	75.70	0.00	24.0
1-B	0.01	98.86	100.00	86.21	77.0
1-C	0.00	16.57	69.07	0.00	18.0
1-D	0.00	0.0	52.53	0.00	3.0
1-E	0.00	0.0	53.20	0.00	2.0
1-F	0.00	58.82	64.60	0.00	0.0
d (Å) ≤	3.3	3.5	3.5	3.8	
A (deg) ≥	150.0	135.0	130.0	140.0	
R^2	0.890	0.514	0.904	0.890	

Table 2. Comparison between the Three Best Computational Protocols P1, P2, and P3 Obtained by Averaging the Theoretical Cross-linking Probability of **1**−**6** DNA Adducts in the SDEM Ensembles versus the Experimental Inhibition Activity with Highest Correlation r^2 [a]

	Boltzmann averaged cross-linking probability p_{A-F} with SDEM in % at 300 K			
DNA adduct	P1	P2	P3	pIC_{50} [b]
1	15.11	16.14	16.31	−0.20
2	16.77	17.03	17.03	0.30
3	42.21	42.21	42.21	2.33
4	33.91	35.55	36.37	2.14
5	1.59	1.59	1.59	−0.64
6	0.14	0.14	0.14	−1.09
r^2	0.961	0.963	0.965	
d in Å ≤	3.5−3.6	3.7−3.8−3.9	4.0	
a in deg ≥	140.0	140.0	140.0	

[a] Filtering conditions are expressed by attack distance *d* and angle *a*. [b] pIC_{50} calculated from IC_{50} in μM concentrations (Figure 1).

The SDEM protocol provided the best correlation factor r^2, with values slightly greater than 0.9. The correspondence was particularly good for the most reactive DNA sequences **A**, **B**, and **C**. The fault in prediction of this method was found with sequence **F**, most likely because the molecular mechanics does not accurately reflect the intrinsic reactivity difference between guanine and the adenine in third position of the duplex DNA.

On the basis of the comparative analysis between the computational methods, the SDEM protocol was adopted for the molecular modeling of the DNA adducts with compounds **2**−**6**. The aim of this second analysis was to find the best computational protocol (distance and angle filtering criterion) that most effectively reproduced the cytotoxic activity trend, expressed as pIC_{50}. Again monoadducts built as in Chart 1 were submitted to the analysis the epoxide methylen carbon − N7 third purine geometry. The best three computational protocols against the available inhibition activities with the square correlation factors are reported in Table 2.

Experiments carried out with other cross-linking agents (data not shown) revealed that this computational approach should be integrated with other methods such as QM/MM and/or QSAR descriptors for a more complete validation. However, despite several approximations of the model, the

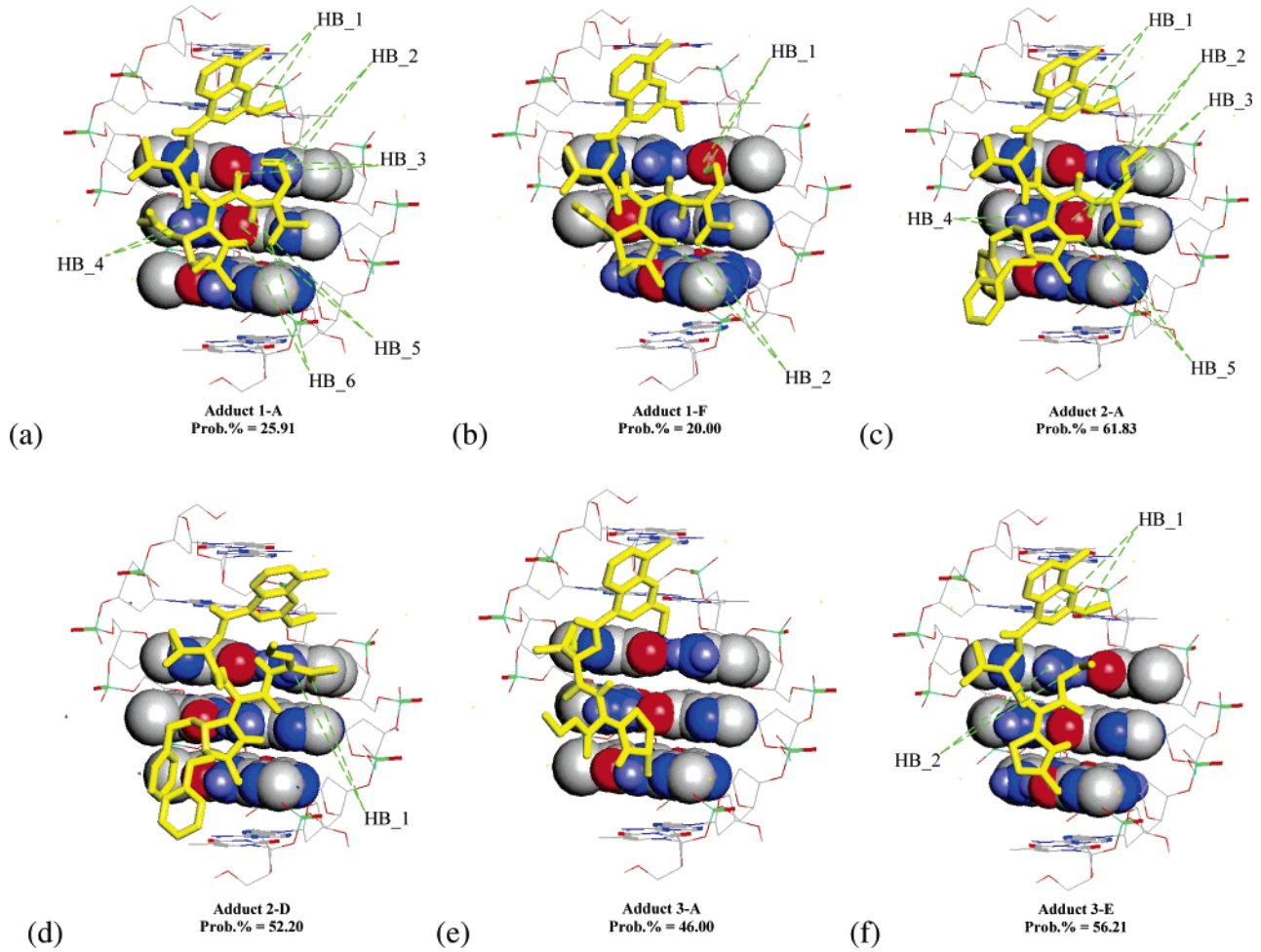

Figure 3. Hydrogen bond network in the SDEM energy minimum most relevant conformers of the **1**-DNA (a, b), **2**-DNA (c, d), and **3**-DNA (e, f) monoadducts. Compounds **1**−**3** are shown as polytube, the reactive triplets are shown with the spacefill, sugars, backbone, and other bases are indicated with wireframe. The dashed lines indicate the compound-DNA hydrogen bond interactions. Na^+ counterions have been omitted. Prob % is the Boltzmann probability at 300 K of each displayed conformation.

computational protocols P1−P3 were able to reproduce with high correlation factors the activity scale of compounds **1**−**6** uniquely basing on the cross-linking probability of the 36 DNA monoadducts. Regarding the filtering criteria, it is interesting to note that the distance *d* resulted less important than the attack angle *a*. Actually distances from 3.5 to 4.0 Å were compatible with high correlation factors, while no tolerance in the attack angle was permitted. The value of 140° or higher seemed to be necessary for deriving a good correlative model.

After the identification of the most appropriate method and filtering conditions, we analyzed the global minimum energy conformations with SDEM method.

As in our previous work[11] the intra- and intermolecular hydrogen bond (HB) analysis of the most populated monoadduct conformers was carried out in order to understand the driving forces for noncovalent interactions between the six DNA sequences and the six compounds. In Figures 3 and 4, major groove view pictures of the most relevant energy minimum conformers have been reported. All other pictures are available in the Supporting Information, Figures 7−9.

1 and 2 DNA Monoadducts. The structural similarity of compounds **1** and **2** makes possible the discussion of the results in this section. The results of the **1**-DNA monoadduct simulations reproduced the geometries of our previous work.[11] In the previous study, we considered only sequences **A**−**D** and highlighted the occurrence of several hydrogen bonding interactions. In the present work we extended our simulations to sequences **E** and **F** (Figure 3). The visual inspection of most stable conformers revealed the highest number of hydrogen bonds in the most cross-linkable **1-A** and **1-B** monoadducts with six hydrogen bonds. Other, less reactive adducts are characterized by a range of HB interactions varying from 5 to 2. This behavior is consequence of the nucleobase character in the fourth and third positions of the duplex DNA segments. Actually, the thymine in the fourth position of sequences **C**, **D**, and **F** is strictly related to the lowest number of hydrogen bonds. Two accompanying effects play an important role for the cross-linking properties of the adducts with **1**. Steric hindrance of the thymidine methyl group crowding against the acetate moiety in 13, and the absence of an amine hydrogen bond donor of other nucleobase sequences **A**, **B**, and **E** that are involved in one hydrogen bond with the sp^3 oxygen in O14 of **1**. Consequently the epoxide ring is pushed relatively far from the purine N7 of the third nucleotide, with an accompanying loss of cross-linking probability. The role of the third nucleotide is particularly important for the sequences **E** and **F**, where the guanine is replaced by the less nucleophilic

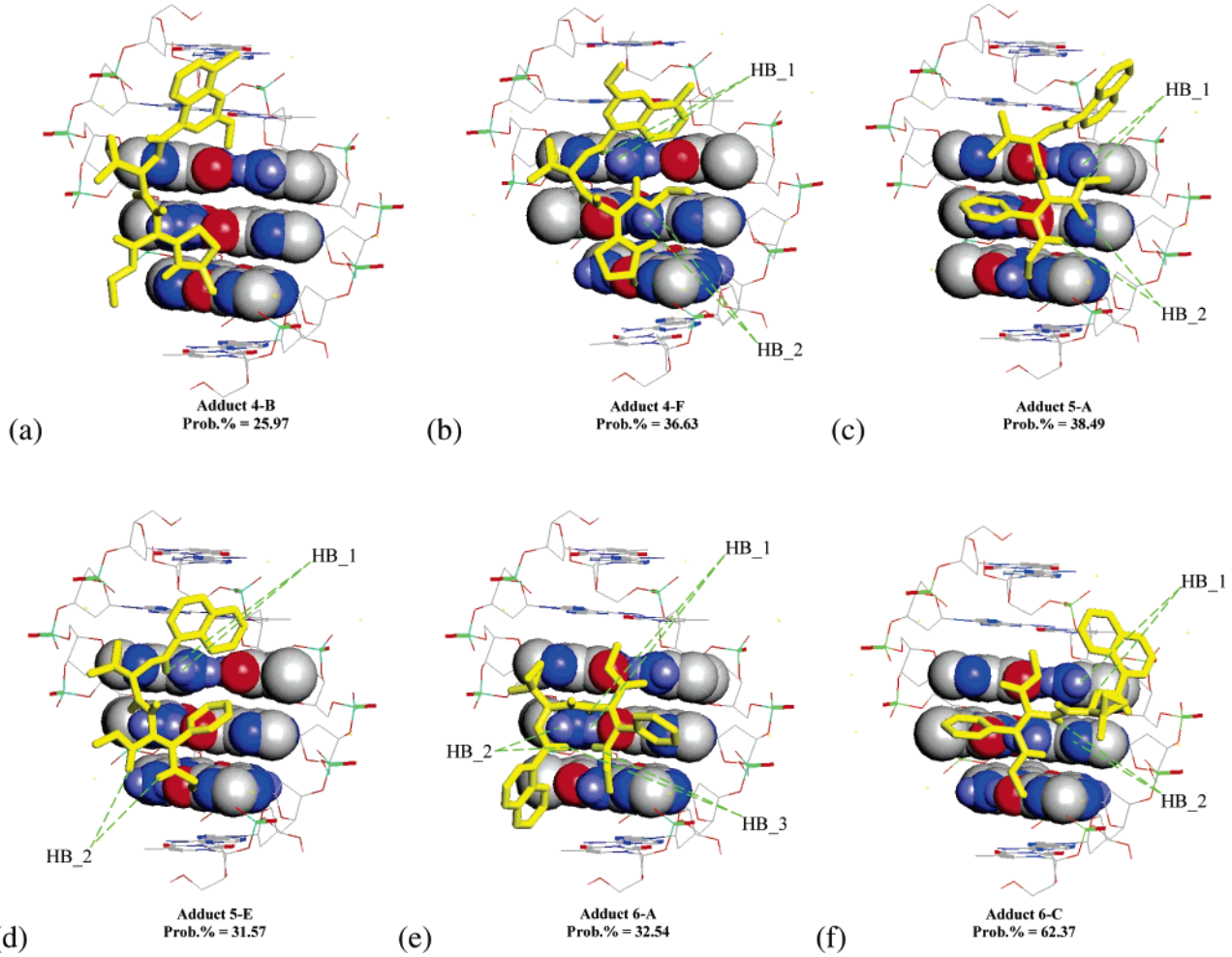

Figure 4. Hydrogen bond network in the SDEM energy minimum most relevant conformers of the **4**-DNA (a, b), **5**-DNA (c, d), and **6**-DNA (e, f) monoadducts. Compounds **4**−**6** are shown as polytube, the reactive triplets are shown with the spacefill, sugars, backbone, and other bases are indicated with wireframe. The dashed lines indicate the compound-DNA hydrogen bond interactions. Na^+ counterions have been omitted. Prob % is the Boltzmann probability at 300 K of each displayed conformation.

adenine base.[22] The different electronic properties of the purine bases, and hence the relative nucleophilicity of guanine versus adenine, is not detectable by the molecular mechanics methods adopted in this study.

Compound **2** showed similar behavior to **1** with the **A**, **B**, and **E** adducts well stabilized by hydrogen bonds. In this case the hydrophobic interactions play a crucial role, largely due to the *O*-benzyl moieties in 12 and 13. The reinforcing steric effects of the two thymine bases in fourth and fifth nucleotides of **D** causes the reduction in the population of the correct epoxide orientation and a modest reduction of cross-linking probability (Figure 3).

The comparison of the results obtained with the three SDEM computational protocols (Table 2) confirmed, in agreement with the IC_{50} data, that compound **2** is slightly more active than **1** even if two bulky benzyl moieties are introduced in the five-membered ring system.

3 and 4 DNA Monoadducts. Compounds **3** and **4** are closely related to each other, differing only in the stereochemistry of the alkene of the azabicycle system (Figure 1). They represent the most interesting of the six selected compounds because they are the most active cytotoxic agents of this series and include important and accessible simplifications of the five-membered ring (loss of acetyl, hydroxyl and benzyl moieties) and the right side chain (2-amino-1,3-dicarbonyl moiety). Thus, they appear to be excellent probes for drug design modifications of the azinomycin structure.

The visual inspection of global minimum energy adducts of **3** and **4** with DNA generally exhibited a low number of hydrogen bonds (maximum 2) and high mobility of the five-membered ring with respect to **1** and **2**.

An unusual rotation of this ring, found in adducts **3-A** (Figure 3) and **4-B** (Figure 4), is associated with a concomitant loss of cross-link probability. Such a conformational characteristic could be explained by the modest interactions between the ethyl ester side chain of both compounds and the DNA major groove. In other words, the simplified right side chain cannot anchor the flexible skeleton of the molecule to the DNA in the azinomycin bioactive conformation.

However, the decreasing cross-linking probabilities with DNA sequences possessing thymine bases in fourth or fifth nucleotides suggest that the absence of any substituents at azinomycin positions 12 and 13 is less important than the right side chain modification. Actually the maximum value of cross-linking probability found with **3-E** and **3-F** adducts was associated with a right side-chain hydrogen bond stabilization with guanine nucleobases in third and ninth positions (Figure 3 and Supporting Information, Figure 8).

The stereochemistry of the azabicycle system is also correlated with the cross-linking ability of analogues **3** and **4**. In particular, the comparison of minimum energy adducts reveals that the azinomycin-like stereochemistry of compound **3** pushes the five-membered ring into a position toward the DNA major groove more effectively than the inverted stereoisomer, thereby increasing the population of the bioactive conformation. The SDEM average theoretical cross-linking probabilities (Table 2) are in agreement with the IC_{50} data and are able to correctly predict the stereoisomer activity differences.

In conclusion, the stereochemistry of the azabicyclic system must be conserved as in the natural compound **1**, and an improvement in the cross-link capabilities of **3** should be reached by the substitution of the ethyl ester with the original azinomycin right side chain.

5 and 6 DNA Monoadducts. Compounds **5** and **6** are isomers of different configurations of the double bond (Figure 1). They show large differences in antitumor activity and both are less potent than **1**. Both **5** and **6** are interesting because they represent simplified analogues of **1**, and the information arising from simulation of their DNA binding could improve the knowledge about the azinomycin structure activity relationships. The differences with respect to **1** are very important: the azabicyclic ring has been replaced by a simple aziridine, the right side chain has been substituted by a methyl ester, and both methyl and methoxy groups located on the naphthoate moiety have been removed.

The analysis of the results of **5** and **6** DNA monoadducts showed a low number of hydrogen bonds (maximum 2) within the major groove. The conformations of the adducts have been significantly influenced by the configuration of the double bond.

The most stable conformations of the **5**-DNA monoadduct (Figure 4) are characterized by the phenyl ring interaction within the major groove, respectively, with the fourth pyrimidines of **A**, **B**, and **C** sequences and the ninth−tenth nucleobases of **D**, **E**, and **F** nucleic acids. In all cases the naphthoate ring location, mimicking that observed in the other active compounds, is in the third−tenth nucleic acid pair, but the epoxide position toward the N7 purine target is not always optimized for a productive cross-link. This affects the overall cross-linking probability, as shown in Table 2.

Conversely, compound **6** displayed a completely different cross-link conformation with respect to the previous azinomycin analogues. In the bioactive conformation of the previous compounds the naphthoate normally interacts with tenth and eleventh nucleotides with hydrogen bonds and/or hydrophobic contacts. Most of the **6**-DNA monoadducts in the global minimum energy conformations locate the naphthoate in front of the fifth nucleotide (Figure 4). The only exception is the very unproductive **6**-**C** adduct with the epoxide significantly more than 10 Å from the N7 target atom. What is interesting to note is that several adducts (**6**-**A**, **6**-**D**, and **6**-**F**) show good compatibility with cross-link formation, demonstrating a second possible bioactive conformation (Figure 4 and Supporting Information, Figure 9). An additional feature of such structures is an intramolecular hydrogen bond bridge between the sp^2 oxygen of the naphthoate ester and the amide NH of the ring-opened aziridine moiety.

Compounds **5** and **6** open a new, interesting strategy for the design of azinomycin analogues. Modeling indicated the crucial role of the C7, C8 double bond in the assumption of the azinomycin-like cross-link conformation. Compound **6** suggested a new cross-link conformation that could be optimized by means of a new analogue design, opening the way for a new related class of anticancer drugs.

CONCLUSIONS

With respect to our previous work[9,10] we have significantly improved and refined our computational model, upgrading the study with the other two DNA sequences **E** and **F**. The availability of quantitative experimental cross-linking data[13] of the natural compound **1** and the six DNA sequences made possible the comparative correlation study using four different computational methods. One of them, the SDEM protocol, yielded results superior to the others and was adopted for the molecular modeling of the **2**−**6** DNA adducts. Taking into account several reasonable approximations, we found a good correlation between the average theoretical cross-linking properties and the cytotoxic activity of compounds **1**−**6**, with three computational protocols providing a systematic exploration of the distance/angle based filtering criterion.

The analysis of the most stable monoadduct conformations revealed some interesting structure−activity relationships. Modifications at C12 and C13 on the five-membered ring of the natural compound increase the theoretical cross-linking ability of the drug analogues. The right side chain of **1** is important for anchoring the drug within the major groove of the DNA. Combining these two pieces of information and keeping the azabicycle stereochemistry at C11 the same as the natural compound is possible to design potentially more active and/or selective azinomycin derivatives. The analysis of the less potent analogue **6** (*Z* stereoisomer) revealed a new cross-linking bioactive conformation that is not related with the azinomycin active conformer.

The computational approach presented in this manuscript is currently in progress for extending the activity prediction to other cross-linking agents strictly not related to the azinomycin scaffold. This specific issue is now under further investigation in our laboratories and will be the object of a future communication.

ACKNOWLEDGMENT

The authors thank the ISN (Istituto di Scienze Neurologiche sezione di Catanzaro) of the CNR (Consiglio Nazionale delle Ricerche) for the computational support and Dr. Mark T. Tierney for helpful suggestions and modifications to the manuscript. This research was supported with funding from NATO (CRG 970160) and the National Institutes of Health (CA 65875). S.A. is grateful to the FIRC for a short-term fellowship (2001) and to the Young Researcher Project of the CNR. For this work F.O. was supported by a fellowship from AIRC.

Supporting Information Available: MC, SD, SDEM, and MCSD details of the **1**-DNA simulations and all pictures of the monoadduct global minimum energy conformers not reported in the manuscript. This material is available free of charge via the Internet at http://pubs.acs.org.

REFERENCES AND NOTES

(1) Nagaoka, K.; Matsumoto, M.; Oono, J.; Yokoi, K.; Ishizeki, S.; Nakashima, T. Azinomycins A and B, New Antitumor Antibiotics. I. Producing Organism, Fermentation, Isolation and Characterization. *J. Antibiot.* **1986**, *39*, 1527−1532. Yokoi, K.; Nagaoka, K.; Nakashima, T. Azinomycins A and B, New Antitumor Antibiotics. II. Chemical Structures. *Chem. Pharm. Bull.* **1986**, *34*, 4554−4461.

(2) Ishizeki, S.; Ohtsuka, M.; Irinoda, K.; Kukita, K. I.; Nagoka, K.; Nakashima, T. Azinomycins A and B, New Antitumor Antibiotics. III. Antitumor Activity. *J. Antibiot.* **1987**, *40*, 60−65.

(3) Hodgkinson, T. J.; Shipman M. Chemical synthesis and mode of action of the azinomycins. *Tetrahedron* **2001**, *57*, 4467−4488. Hashimoto, M.; Matsumoto, M.; Yamada, K.; Terashima, S. Synthetic studies of carzinophilin. Part 4: Chemical and biological properties of carzinophilin analogues. *Tetrahedron* **2003**, *59*, 3089−3097.

(4) For a review on DNA cross-linking agents, see: Rajski, S. R.; Williams, R. M. DNA Cross-Linking Agents as Antitumor Drugs. *Chem. Rev.* **1998**, *98*, 2723−2795.

(5) Fujiwara, T.; Saito, I.; Sugiyama, H. Highly Efficient DNA Interstrand Cross-linking Induced by an Antitumor Antibiotic, Carzinophilin. *Tetrahedron Lett.* **1999**, *40*, 315−318.

(6) Armstrong, R. W.; Salvati, M. E.; Nguyen, M. Novel Interstrand Cross-Links Induced by the Antitumor Antibiotic Carzinophilin/Azinomycin B. *J. Am. Chem. Soc.* **1992**, *114*, 3144−3145.

(7) Coleman, R. S. Issues of Orthogonality and Stability: Synthesis of the Densely Functionalized Heterocyclic Ring System of the Antitumor Agents Azinomycins A and B. *Synlett* **1998**, *10*, 1031−1039.

(8) Coleman, R. S.; Li, J.; Navarro, A. Total Synthesis of Azinomycin A. *Angew. Chem., Int. Ed.* **2001**, *40*, 1736−1739. Coleman, R. S.; Kong, J. S.; Richardson, T. E. Synthesis of Naturally Occurring Antitumor Agents: Stereocontrolled Synthesis of the Azabicyclic Ring System of the Azinomycins. *J. Am. Chem. Soc.* **1999**, *121*, 9088−9095. Coleman, R. S.; Richardson, T. E.; Carpenter, A. J. Synthesis of the Azabicyclic Core of the Azinomycins: Introduction of Differentiated *trans*-Diol by Crotylstannane Addition to Serinal. *J. Org. Chem.* **1998**, *63*, 5738−5739. Coleman, R. S.; Kong, J. S. Stereocontrolled Synthesis of the Fully Elaborated Aziridine Core of the Azinomycins. *J. Am. Chem. Soc.* **1998**, *120*, 3538−3529. Coleman, R. S.; Carpenter, A. J. Synthesis of the Aziridino[1,2-*a*]pyrrolidine Substructure of the Antitumor Agents Azinomycin A and B. *J. Org. Chem.* **1992**, *57*, 5813−5815.

(9) Alcaro, S.; Coleman, R. S. Molecular Modeling of the Antitumor Agents Azinomycins A and B: Force-Field Parametrization and DNA Cross-Linking Based Filtering. *J. Org. Chem.* **1998**, *63*, 4620−4625.

(10) Alcaro, S.; Coleman, R. S. A Molecular Model For DNA Cross-Linking By The Antitumor Azinomycin B. *J. Med. Chem.* **2000**, *43*, 2783−2788.

(11) Alcaro, S.; Ortuso, F.; Coleman, R. S. DNA Cross-Linking by Azinomycin B: Monte Carlo Simulations in the Evaluation of Sequence Selectivity. *J. Med. Chem.* **2002**, *45*, 861−870.

(12) Coleman, R. S.; Burk, C. H.; Navarro, A.; Brueggemeier, R. W.; Diaz-Cruz, E. S. Role of the Azinomycin Naphthoate and Central Amide in Sequence-Dependent DNA Alkylation and Cytotoxicity of Epoxide-Bearing Substructures. *Org. Lett.* **2002**, *4*, 3545−3548.

(13) Coleman, R. S.; Perez, R. J.; Burk, C. H.; Navarro, A. Studies on the Mechanism of Action of Azinomycin B: Definition of Regioselectivity and Sequence Selectivity of DNA Cross-Link Formation and Clarification of the Role of the Naphthoate. *J. Am. Chem. Soc.* **2002**, *124*, 13008−13017.

(14) The three discarded monoadducts are as follows: MAT = monoalkylation aziridine top; MEB = monoalkylation epoxide bottom; MET = monoalkylation epoxide top.

(15) Mohamadi, F.; Richards, N. G. J.; Guida, W. C.; Liskamp, R.; Lipton, M.; Caufield, C.; Chang, G.; Hendrickson, T.; Still, W. C. MacroModel − An Integrated Software System for Modeling Organic and Bioorganic Molecules Using Molecular Mechanics. *J. Comput. Chem.* **1990**, *11*, 440−467.

(16) *MacroModel ver 7.2*, Schrödinger Inc., Portland, OR, 1998−2001.

(17) This force constant value is the default value suggested by the MacroModel setup procedure.

(18) Since MacroModel version 7.2 energy treatment of constrained systems is different from that of version 5.5 used in our previous work, we added the directive DEBG 17 that allows the new version of the program to energy evaluate the conformers with the original method.

(19) MC method: Chang, G.; Guida, W. C.; Still, W. C. An Internal Coordinate Monte Carlo Method for Searching Conformational Space. *J. Am. Chem. Soc.* **1989**, *111*, 4379−4386. MCSD method: Guarnieri, F.; Still, W. C. A Rapidly Convergent Simulation Method: Mixed Monte Carlo/Stochastic Dynamics. *J. Comput. Chem.* **1994**, *15*, 1302−1310.

(20) The distance between the methylene carbon and the N7 purine was varied between 3 and 4 Å with a 0.1 Å step. The attack angle, measured considering the epoxide oxygen, the epoxide methylene carbon and the N7 purine nitrogen of the third nucleotide, was varied from 90 to 150 deg with a 5 deg step.

(21) Alcaro, S.; Arena, A.; Neri, S.; Ottanà, R.; Ortuso, F.; Pavone, B.; Vigorita, M. G. Design and synthesis of DNA-intercalating 9-fluoren-β-O-glycosides as potential IFN-inducers, and antiviral and cytostatic agents. *Bioorg. Med. Chem.* **2004**, *12*, 1781−1791.

(22) Sugiyama, H.; Saito, I.; Sugiyama, H. Theoretical Studies of GG-Specific Photocleavage of DNA via Electron Transfer: Significant Lowering of Ionization Potential and 5′-Localization of HOMO of Stacked GG Bases in B−Form DNA. *J. Am. Chem. Soc.* **1996**, *118*, 7063−7068. Senthilkumar, K.; Grozema, F. C.; Fonseca Guerra, C.; Bickelhaupt, F. M.; Siebbeles, L. D. A. Mapping the Sites for Selective Oxidation of Guanines in DNA. *J. Am. Chem. Soc.* **2003**, *125*, 13658−13659.

CI0496595